(23) Lefebvre, D.; Jasse, B.; Monnerie, L. *Polymer* **1983**, *24*, 1240.
(24) Lee, A.; Wool, R. P. *Macromolecules* **1986**, *19*, 1063.
(25) Lee, A.; Wool, R. P. *Macromolecules* **1987**, *20*, 1924.
(26) Bates, F. S.; Dierker, S. B.; Wignall, G. D. *Macromolecules* **1986**, *19*, 1938.
(27) Buckingham, A. D.; Hentschel, H. G. E. *J. Polym. Sci., Polym. Phys. Ed.* **1980**, *18*, 853.
(28) Doi, M.; Edwards, S. F. *The Theory of Polymer Dynamics*; Clarendon: Oxford, 1986.
(29) Doi, M. *J. Non-Newtonian Fluid Mech.* **1987**, *23*, 151.
(30) Kuhn, W.; Grün, F. *J. Polym. Sci.* **1946**, *1*, 183.
(31) Michl, J.; Thulstrup, E. W. *Spectroscopy with Polarized Light*; VCH: New York, 1986.
(32) Matsuoka, Y. *J. Phys. Chem.* **1980**, *84*, 1361.
(33) Schmidt, P.; Schneider, B. *Makromol. Chem.* **1983**, *184*, 2075.
(34) Jacobi, M. M.; Stadtler, R.; Gronski, W. *Macromolecules* **1986**, *19*, 2884.
(35) Sotta, P.; Deloche, B.; Herz, J.; Lapp, A.; Durand, D.; Rabadeux, J.-C. *Macromolecules* **1987**, *20*, 2769.
(36) Queslel, J.-P.; Erman, B.; Monnerie, L., to be submitted for publication.
(37) Jarry, J.-P.; Monnerie, L. *Macromolecules* **1979**, *12*, 316.
(38) Merrill, W. W.; Tirrell, M., to be submitted for publication.
(39) Doi, M.; Pearson, D. S.; Kornfield, J.; Fuller, G. G., to be submitted for publication.
(40) Johnson, S. J.; Frattini, P. L.; Fuller, G. G. *J. Colloid Interface Sci.* **1985**, *104*, 440.
(41) Lodge, A. S.; Meissner, J. *Rheol. Acta* **1972**, *11*, 351.
(42) Osaki, K.; Kimura, S.; Kurata, M. *J. Polym. Sci., Polym. Phys. Ed.* **1981**, *19*, 517.
(43) Leonov, A. I. *Rheol. Acta* **1976**, *15*, 85.
(44) Azzam, R. M. A.; Bashara, N. M. *Ellipsometry and Polarized Light*, North-Holland: Amsterdam, The Netherlands, 1987.
(45) Morton, M.; Fetters, L. J. *Rubber Chem. Technol.* **1975**, *48*, 359.
(46) Rachapudy, H.; Smith, G. G.; Raju, V. R.; Graessley, W. W.; *J. Polym. Sci., Polym. Phys. Ed.* **1979**, *17*, 1211.
(47) Pearson, D. S.; Kiss, A. D.; Kornfield, J. A.; Fuller, G. G., to be submitted for publication.
(48) Laun, H. M. *Rheol. Acta* **1978**, *17*, 1.
(49) Pearson, D. S.; Rochefort, W. E. *J. Polym. Sci., Polym. Phys. Ed.* **1982**, *20*, 83.
(50) Fukuda, M.; Wilkes, G. L.; Stein, R. S. *J. Polym. Sci., Polym. Phys. Ed.* **1971**, *9*, 1417.
(51) Bouë, F.; Farnoux, B.; Bastide, J.; Lapp, A.; Herz, J.; Picot, Cl. **1986**, *1*, 637.

Local Segmental Dynamics of Polyisoprene in Dilute Solution: Solvent and Molecular Weight Effects

Dean A. Waldow, Brian S. Johnson, Patrick D. Hyde, and M. D. Ediger*

Department of Chemistry, University of Wisconsin, Madison, Wisconsin 53706

Toshiaki Kitano† and Koichi Ito

Department of Materials Science, Toyohashi University of Technology, Toyohashi 440, Japan. *Received June 14, 1988; Revised Manuscript Received August 19, 1988*

ABSTRACT: A picosecond holographic grating technique has been utilized to observe the solvent and molecular weight dependence of the local segmental dynamics of anthracene-labeled polyisoprene in dilute solution. Solvent quality influences the local dynamics by changing the local segment concentration in the vicinity of the labeled segment. The local dynamics in a Θ solvent exhibited a molecular weight dependence not observed in good solvents. The shape of the orientation autocorrelation function was constant under all conditions investigated. These results are consistent with the hypothesis that local segmental dynamics in dilute solution depend only upon solvent viscosity and solvent thermodynamic power.

I. Introduction

The local segmental dynamics of polymer chains have a strong influence on the macroscopic properties of polymeric systems. In polymer solutions where local dynamics occur on picosecond and nanosecond time scales, this influence is mainly through the larger distance scale motions which dominate ordinary viscoelastic properties under these conditions. Because dynamics on the length scale of a few monomer units are strongly dependent upon the details of the monomer structure, information about local segmental dynamics provides an important intermediate link between molecular structure and larger motions. In a polymer melt near T_g, the time scales for local conformational transitions slow dramatically. It is widely held that the quenching of backbone conformational transitions is intimately connected with the glass transition. Certain types of local segmental dynamics can also directly influence material properties in the sub-T_g region. Given the fundamental significance of local segmental dynamics, it is not surprising that a wide variety of experimental techniques have been utilized in their investigation in recent years. Among these are dielectric relaxation,[1] NMR,[2] dynamic light scattering,[3] ESR,[4] and optical spectroscopic techniques.[5-13]

In every experimental measurement of local segmental dynamics, both the molecular structure of the polymer and the environment of the chains contribute to the observed dynamics. The contribution of the environment must be thoroughly understood before progress can be made on the question of how the structure influences the dynamics. One question of particular interest is the extent to which the local chemical details of solvent–polymer interactions must be considered. Since local segmental dynamics occur on about the same length scale as the dimensions of solvent molecules, it is not obvious that the effect of the solvent on the local dynamics will be adequately described by bulk properties. Indeed, the reorientation of small solute molecules even in simple solvents is known to be strongly influenced by solvent–solute interactions.[14]

In this paper we focus our attention on the influence of solvent, temperature, and molecular weight on the local segmental dynamics of polyisoprene in dilute solution. A transient holographic grating technique was utilized to observe the orientation autocorrelation function of a backbone bond in anthracene-labeled polyisoprene. The anthracene chromophore was covalently bonded into the chain such that the transition dipole for the lowest electronic excited state lies along the chain backbone. This

† Current address: Polyplastics Co., Ltd., 973 Miyajima, Fuji-City, Shizuoka-Pref. 416, Japan.

0024-9297/89/2222-1345$01.50/0

Table I
Polymer Characterization

	M_n	M_w/M_n	%cis	%trans	%3,4-vinyl
PIP-10	10800	1.16	39	36	25
PIP-100	104000	1.09	54	36	10
PIP-300	302000	1.10	43	45	12

ensures that only backbone motions are detected. Because the entire time dependence of the orientation autocorrelation function is measured, local segmental dynamics under a wide range of conditions can be unambiguously compared.

Our major conclusion in this paper is that it is possible to explain the local segmental dynamics of polyisoprene in a range of solvents by considering only two bulk properties: solvent viscosity and solvent thermodynamic quality. Scaling the observed correlation times for local dynamics by the solvent viscosities reduces the range of results to a common value within about 60%. The remaining variation can be explained by differences in solvent power. Solvent power affects local dynamics through changes in the global chain configuration. The expanded chains found in good solvents give rise to faster dynamics because individual chain segments are in less congested environments on the average. Supporting evidence for this argument is found in the molecular weight dependence of the local segmental dynamics in good and Θ solvents. In good solvents, no molecular weight dependence is observed, while a definite molecular weight dependence is seen in a Θ solvent. These effects are successfully modeled by random walk calculations utilizing regular and self-avoiding walks to model the statistics of polymer chains in Θ solvents and good solvents, respectively. The shapes of the observed correlation functions were identical for all the conditions we investigated. This provides additional evidence that the basic mechanism of local conformational dynamics does not change from solvent to solvent.

II. Experimental Section

Materials. Anthracene-labeled polyisoprene chains were prepared anionically such that each chain contains one chromophore approximately in the chain center.[5] The structure of the labeled chain is shown in Figure 1. Chain microstructures and molecular weights are summarized in Table I. Solvents used in these experiments were 2-pentanone (97%, Aldrich), toluene (Aldrich spectroscopic grade), hexane (Aldrich Gold label), cyclohexane (Aldrich Gold label), and chlorobenzene (Aldrich Gold label). Solvent viscosities for temperatures greater than 0 °C are from ref 15. Viscosities for lower temperatures were measured with a Cannon-Fenske viscometer. All solvents were used as received except for 2-pentanone which was treated to remove trace UV-absorbing impurities. The Θ temperature for 2-pentanone is estimated at 43 °C from reported values for polyisoprene chains with various microstructures.[16] All solutions were degassed to remove oxygen through multiple freeze–pump–thaw cycles. For all polymer solutions, the optical densities at the origin $S_0 \rightarrow S_1$ transition (403.5 nm) ranged from 0.08 to 0.20. The chromophore concentrations were low enough that the contribution of energy transfer to the anisotropy decay could be neglected. The solution concentrations for the experiments ranged up to 10% w/w. Consistent with previous studies, no dependence of the local dynamics on concentration was noted in this range.[2a,8] For the purpose of this paper, these solutions will be referred to as dilute. Thermal degradation was not observed except for the PIP-300/2-pentanone solution at 75 °C where the measured correlation times were somewhat less reproducible than for the lower temperature experiments.

Experimental Technique. The transient holographic grating technique utilized in these experiments has been fully described elsewhere.[5] The experiment observable for this technique is the orientation autocorrelation function. This function represents the time-dependent motion of the transition dipole of the anthracene chromophore. Because the anthracene molecule is covalently bonded in the chain backbone with its transition dipole along the backbone, the motion of the label directly reflects conformational changes in the chain.

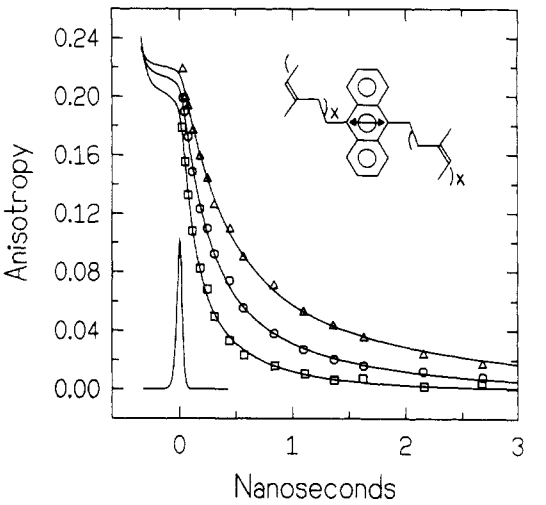

Figure 1. Time-dependent anisotropies for PIP-300 labeled polyisoprene in 2-pentanone. The anisotropy function shows how the initial orientation provided by photoselection decays in time due to local conformational dynamics. The symbols represent the experimental anisotropies, and the lines are the best fit curves using the Hall–Helfand correlation function at temperatures of 23 °C (△), 36 °C (○), and 56 °C (□). The impulse response function for the laser system is shown and has a FWHM of ~50 ps. The structure of the labeled polyisoprene is shown as an inset. The double-headed arrow shows the orientation of the transition dipole.

In the transient grating technique, two vertically polarized laser beams are crossed such that their optical interference creates a spatially periodic intensity pattern in an absorbing sample. This results in a spatial grating of excited states which acts to diffract a third (probe) beam brought into the sample at some later time. The intensity of the diffracted signal is measured for the probe beam polarized parallel ($T_\parallel$) and perpendicular ($T_\perp$) to the polarization of the excitation beam. Conceptually, the excitation pulses photoselect an anisotropic subset of transition dipoles. The probe pulse then monitors the time evolution of the randomization of these transition dipoles (due to polymer backbone motions).

From the transient grating signals, the time-dependent anisotropy function can be calculated:

$$r(t) = \frac{(T_\parallel(t))^{1/2} - (T_\perp(t))^{1/2}}{(T_\parallel(t))^{1/2} + 2(T_\perp(t))^{1/2}} \quad (1)$$

The time-dependent anisotropy is directly related (within a multiplicative constant) to the orientation autocorrelation function CF(t) through

$$r(t) = r(0)\mathrm{CF}(t) \quad (2)$$

where $r(0)$ is the fundamental anisotropy of the transitions being utilized.

Data Analysis. The Hall–Helfand model of the correlation function[17]

$$\mathrm{CF}(t) = \exp(-t/\tau_1)\exp(-t/\tau_2)I_0(t/\tau_1) \quad (3)$$

was used as a convenient model for fitting the experimental anisotropy curves. An iterative reconvolution technique was utilized to fit $r(t)$ to three parameters: $r(0)$, τ_1, and τ_2. Typical anisotropy curves are shown in Figure 1. The sample is PIP-300 polyisoprene in toluene at −22, 22, and 56 °C. The symbols represent the experimental points, and the smooth curves are the best fit with the Hall–Helfand function. The ratio of time constants from the Hall–Helfand fits for all conditions investigated in this paper was $\tau_2/\tau_1 = 4.4 \pm 1.4$. Since the shapes of all measured correlation functions were approximately the same, we can characterize each correlation function with a single decay parameter for the purpose of further analysis. The correlation time[18]

$$\tau_c = \int_0^\infty CF(t)\, dt \tag{4}$$

was used for this purpose. For the Hall–Helfand function, this integral yields

$$\tau_c = \left\{ \frac{2}{\tau_1 \tau_2} + \frac{1}{\tau_2^2} \right\}^{-1/2} \tag{5}$$

We utilized τ_c to analyze the data rather than τ_1 or τ_2 because this resulted in somewhat less scatter in the resulting plots.

Correction for End-over-End Motion. The two major physical processes that contribute to the anisotropy decay are internal bond rotation (local segmental dynamics) and overall molecular rotation. In order to focus on local segmental dynamics, we need to correct the data to eliminate the slight influence of overall rotation. The end-over-end reorientation time is given by

$$\tau_{EOE} = \gamma \frac{M[\eta]\eta_0}{RT} \tag{6}$$

where M is the molecular weight, $[\eta]$ is the intrinsic viscosity, η_0 is the solvent viscosity, R is the gas constant, and T is temperature in kelvin. The intrinsic viscosities were taken from the literature.[19] The constant γ has been experimentally determined by Bauer et al. to be 0.24 for polystyrene.[20] We used this value of γ in eq 6 to correct the experimental anisotropy data for the effects of end-over-end motion. The correction was applied by noting that

$$CF_{Fit}(t) = CF_{LD}(t) e^{-t/\tau_{EOE}} \tag{7}$$

Here we designate the observed correlation function as CF_{Fit} and the correlation function characteristic of local dynamics alone as CF_{LD}. By applying eq 7, the fitted value of τ_2 is modified to extract the corrected time constant, $\tau_{2,corr}$:

$$\tau_{2,corr} = \left\{ \frac{1}{\tau_2} - \frac{1}{\tau_{EOE}} \right\}^{-1} \tag{8}$$

The corrected correlation time is then calculated from τ_1 and $\tau_{2,corr}$. The correction to τ_c for the PIP-10 results ranged from 5% to 13%. The correction was not applied to the PIP-100 and PIP-300 results because it was negligible. The data presented in this paper are shown with the results for PIP-10 corrected, except in Figure 6. Correction of the data with other values of γ suggested by theoretical calculations[21] would not qualitatively change the appearance of any of the figures.

III. Results and Discussion

Good Solvent. In Figure 1, anisotropy data are shown for PIP-300 in toluene at temperatures of −22, 22, and 55 °C. These data are typical for the transient grating experiments we have performed. The experimental points are shown as symbols, while the smooth lines represent the best fit of the data using the Hall–Helfand correlation function. Also shown in Figure 1 is the instrumental response function for our experimental setup. The narrow instrumental response function (FWHM ≈ 50 ps) is needed to adequately resolve the very rapid local segmental dynamics of polyisoprene. The structure of the anthracene-labeled polyisoprene used in these experiments is shown as an inset in Figure 1.

Figure 2 illustrates the effect of molecular weight and temperature on the local segmental dynamics of polyisoprene in a good solvent. In this figure, data from samples PIP-10 and PIP-300 in toluene are plotted in an Arrhenius format. Each symbol represents an independent measure of the correlation time from an anisotropy curve like those shown in Figure 1. The lines are linear least-squares fits to the data. The slopes of these lines are proportional to the activation energy for local conformational transitions.

The correlation functions we observe for the PIP-10 sample are slightly influenced by whole molecule tumbling. This end-over-end rotation is negligible for the higher molecular weight samples. As discussed in section II, the data in Figure 2 have been corrected such that they accurately represent correlation times for local polymer motion. Within experimental errors, there is no difference between the observed local dynamics for the two molecular weights. The activation energy of the local polymer motions for the two molecular weights is 6.4 ± 1.0 kJ/mol. This number is in reasonable agreement with the barrier to rotation of the carbon–carbon single bond in propene: 8.3 kJ/mol.[22]

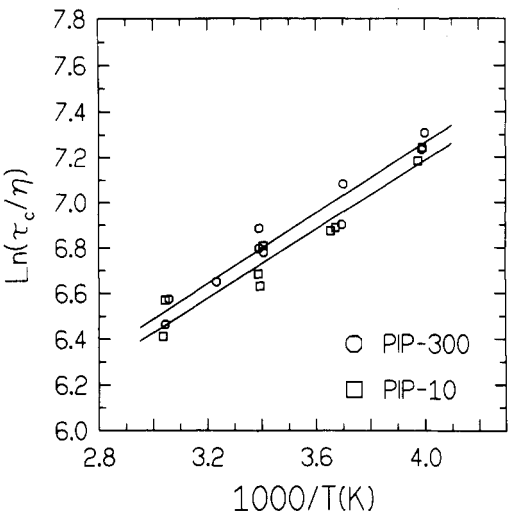

Figure 2. Reduced correlation times for the local segmental dynamics of anthracene-labeled polyisoprene in toluene, a good solvent, plotted in an Arrhenius format: PIP-300 (○) and PIP-10 (□). Each symbol represents an independent measurement of the anisotropy function. τ_c and η are in units of picoseconds and centipoise, respectively. The lines represent the best least-squares fit to the data (higher line for PIP-300). Within experimental error, the local segmental dynamics of polyisoprene are independent of molecular weight in this good solvent.

Θ Solvent. In a previous communication,[23] we presented experiments on the local segmental dynamics of polyisoprene in a Θ solvent. These data are presented here in order to contrast the behavior of local segmental dynamics in good and Θ solvents. In Figure 3, data are shown for PIP-10, PIP-100, and PIP-300 in 2-pentanone. The Θ temperature for the labeled chains in 2-pentanone is about 43 °C and is indicated in the figure. The data from PIP-10 have been corrected for end-over-end motion. Two sets of points were not used in linear fits to the data. The −26 °C data for the PIP-10 sample were not used because the sample was very near phase separation, while the PIP-300 data at 74 °C were not used because of a lack of reproducibility associated with thermal degradation. Linear fits to the data were utilized simply to aid the eye in viewing and are not meant to imply that the data should or actually does follow this form.

Comparison of Good and Θ Solvent Behavior. In order to compare the local segmental dynamics of polyisoprene in good and Θ solvents, we reproduce the results shown in Figures 2 and 3 on a single plot in Figure 4. To avoid confusion, we show only the lines which ran through the data points in those figures (2-pentanone, upper solid lines; toluene, dashed lines). Also shown in the figure are results from a dilute solution of PIP-100 in chlorobenzene (a good solvent) and a linear fit to these data. Notice that the correlation times have been scaled by the viscosities of the solvents. The chlorobenzene results are essentially identical with the toluene data after this scaling (before scaling, the correlation times differed by 30%).

When the data from these three solvents are compared, a number of observations can be made: (1) The local

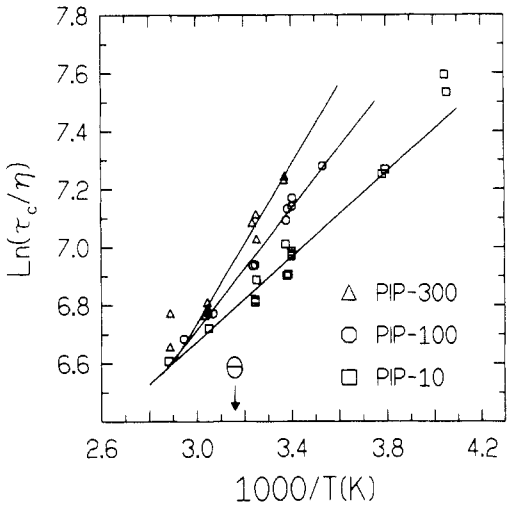

Figure 3. Reduced correlation times for the local segmental dynamics of anthracene-labeled polyisoprene in 2-pentanone, a Θ solvent, plotted in an Arrhenius format: PIP-300 (Δ), PIP-100 (○), and PIP-10 (□). The Θ temperature of 43 °C is indicated. Each data point represents an independent measurement of the correlation function. The lines represent the best least-squares fit to the data (see text). Both the correlation times and the apparent activation energies are molecular weight dependent in this Θ solvent.

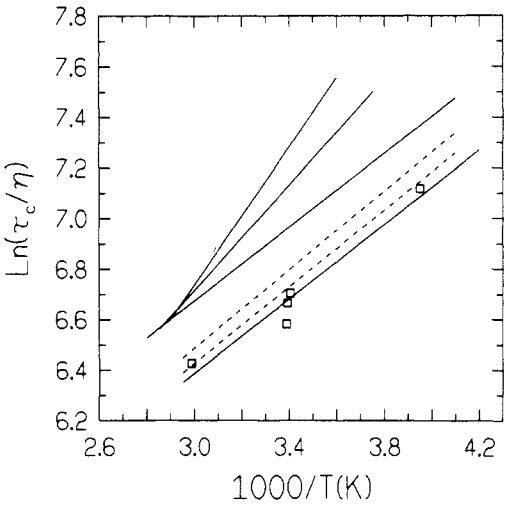

Figure 4. Comparison of reduced correlation times for local segmental dynamics of polyisoprene in good and Θ solvents. The solid lines near the top of the graph are the best fit lines for the Θ solvent, 2-pentanone. The dashed lines are the best fit lines for toluene, a good solvent. Reduced correlation times for PIP-100 in a second good solvent, chlorobenzene (□), are shown with a linear fit to the data. Within experimental error, the chlorobenzene data are not distinguishable from the toluene data. The different behavior of the good and Θ solvents can be explained by considering the average segment density about the labeled segment (see text).

segmental dynamics of polyisoprene in the Θ solvent are slower than in the good solvents. (2) The correlation times for local segmental dynamics increase with molecular weight in a Θ solvent and are essentially independent of molecular weight in good solvents. (3) The apparent activation energy (proportional to the slope) is independent of molecular weight in the good solvents, while in the Θ solvent the apparent activation energy increases with increasing molecular weight. (4) The difference in correlation times between good and Θ solvents is more pronounced for high molecular weight samples than low molecular weight samples.

All of these observations can be explained by considering the local segment concentration about the labeled segment (at the chain center). We assume that an increase in this local segment concentration leads to slower dynamics, presumably because the more rigid environment inhibits local conformational transitions. (It is well-known that increasing the bulk concentration slows local dynamics.[8]) The first observation that good solvent dynamics are faster than Θ solvent dynamics is simply explained by this concept. Since chains expand in good solvents, the immediate environment of the labeled segment will have a larger fraction of solvent in a good solvent than in a Θ solvent, and the dynamics should be correspondingly faster. The second observation noted that correlation times increase with molecular weight in a Θ solvent but are independent of molecular weight in a good solvent. In a previous publication, we explained the Θ solvent result by showing that the local segment concentration increases with molecular weight under Θ conditions.[23] A simple calculation utilizing a Gaussian segment–segment distribution function allows the estimation of the increase in the local concentration with molecular weight. The molecular weight independence of the local dynamics under good solvent conditions is due to excluded volume interactions which tend to keep segments which are far apart along the chain contour far separated in space. Hence, under good solvent conditions, the local concentration is essentially independent of molecular weight.

The third observation about the apparent activation energies can also be explained by the concept of local segment concentration. Chain expansion in the vicinity of the Θ point can lead to an increased apparent activation energy. The activation energy due to internal rotational potentials is supplemented by an additional temperature dependence in the dynamics due to a change in the local segment concentration (because of chain expansion). This second contribution to the temperature dependence increases in strength with increasing molecular weight since global chain expansion becomes more pronounced with higher molecular weights. The apparent activation energy in a *good* solvent should not be a function of molecular weight since average chain configuration does not change appreciably with temperature in a good solvent. This explanation indicates that the activation energy observed in a good solvent should represent the true activation energy associated with the rotational barriers traversed in a local conformational change. Also consistent with this explanation is the observation that the PIP-10 sample in the Θ solvent shows the same activation energy as all molecular weights in the good solvents. This chain is short enough that a substantial change in chain dimensions does not occur over the temperature range studied. The final observation noted that the difference in correlation times between good and Θ solvents increased with molecular weight. As solvent quality increases, chain expansion is most significant for high molecular weight chains. Thus, the change in the rate of local dynamics in going from a Θ solvent to a good solvent should be most pronounced for high molecular weight chains.

In Figure 5 we show random walk calculations which support the explanations given above. A self-avoiding random walk[24] was used to model good solvent statistics, while a regular random walk was used to model Θ conditions.[25] In each case, a three-dimensional cubic lattice was utilized with the lattice spacing equal to the statistic segment length for polyisoprene (16.5 Å). The density of segments in the region around the center segment was calculated for both random and self-avoiding walks as a function of molecular weight. For each complete walk, we recorded the number of segments in a volume defined by

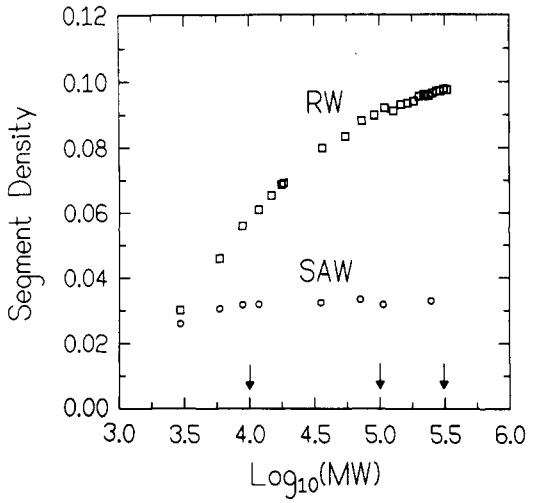

Figure 5. Calculation of the local segment density about the center segment for a polyisoprene chain in a good solvent (self-avoiding random walk, SAW) and a Θ solvent (random walk, RW). The segment density is expressed as a fraction of bulk density. The three molecular weights utilized in this study are indicated with arrows. At all three molecular weights, the segment density is lower for the good solvent, leading to the faster dynamics observed in Figure 4. The molecular weight dependence of the local segment density in a Θ solvent leads to the observed molecular weight dependence of the correlation times.

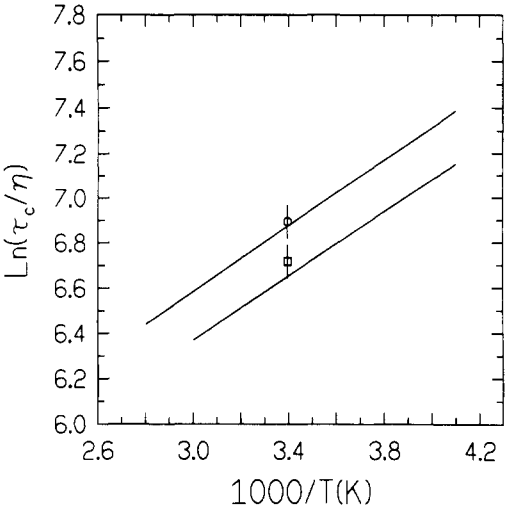

Figure 6. Reduced correlation times for the PIP-10 sample in four solvents of varying thermodynamic quality. The top line is the best fit line to the 2-pentanone data, while the bottom line represents the toluene data. Also shown are data points for hexane (○) and cyclohexane (□). Correcting the correlation times by the viscosities (which vary by a factor of 3) produces reduced correlation times which vary by only 25%. The remaining variations are consistent with differences in solvent quality (see text).

a cube three lattice spacings on a side, centered around the middle chain segment. The center segment itself was excluded from the count. After many walks, we calculated the average segment density about the center segment. These results are shown in Figure 5, with the segment density presented as a fraction of the density of bulk polyisoprene. Arrows along the abscissa indicate the molecular weights utilized in these experiments.

Figure 5 is useful for illustrating several of the points which we have made previously. (1) We noted that the good solvent dynamics were faster than the Θ solvent dynamics. Figure 5 indicates that the self-avoiding walk (good solvent model) shows a less congested environment than the random walk (Θ solvent model) for all molecular weights. (2) The dynamics at the Θ point were molecular weight dependent, while the good solvent dynamics were approximately independent of molecular weight. Figure 5 shows that the local segment concentration has the same behavior. The molecular weight dependence of the local segment concentration under Θ conditions has been verified with an analytical model in a previous publication.[23] (3) The largest change in local dynamics with solvent quality occurs for high molecular weight polymers. It can be seen from Figure 5 that the largest difference in the local segment concentration also occurs at high molecular weight.

It should be emphasized that we do not expect Figure 5 to be quantitatively accurate. The applicability of self-avoiding random walk statistics to short chains or short chain segments is questionable since excluded volume interactions act most strongly on larger length scales.[26] Nevertheless, we expect the qualitative interpretations drawn from Figure 5 to be correct. It is also worth emphasizing that in this section we have considered the local segment concentration about a given segment and not the segment concentration about the center-of-mass of the chain. It is well-known that the latter quantity *decreases* with increasing molecular weight.

One objection which can be raised to the explanation of Figure 4 presented above is that the PIP-10 sample (M_n = 10800) must undergo sufficient chain expansion in going from a Θ solvent to a good solvent for the rate of local dynamics to increase by 25%. This seems like a large effect for such a low molecular weight polymer. In Figure 6, we present data on this sample in four solvents: 2-pentanone, hexane, toluene, and cyclohexane. The corresponding Mark–Houwink coefficients for the molecular weight dependence of the intrinsic viscosity are 0.50, 0.56, 0.67, and 0.70, respectively, for polyisoprene in these solvents.[19] The exact order indicated by these coefficients is not followed in the data, but the figure shows that polyisoprene in the two poorest solvents has the slowest local dynamics, while the two better solvents yield faster dynamics. Given experimental errors, this tends to lend further support to the notion that solvent quality is primarily responsible for the observed differences in τ_c/η. In the absence of viscosity scaling, these differences due to solvent quality would not be apparent. The reduced correlation times vary by 25% at room temperature, while the correlation times without viscosity scaling vary by a factor of 3.

Some aspects of the experimental observations presented in this section have been observed by previous investigators. The result that Θ solvent dynamics tend to be slower than good solvent dynamics has been noted in NMR experiments[27] and in experiments by Valeur et al.[9] utilizing time-resolved optical spectroscopy. These investigators explained their results in a manner consistent with our explanation. Bullock et al. performed ESR on spin-labeled polystyrenes of various molecular weights.[4] They reported an increase in the activation energy as a function of increasing molecular weight in a Θ solvent. However, since these results were not corrected for end-over-end motions, it is difficult to quantitatively compare them to our results. Bullock et al. noted a difference in the activation energy for a high molecular weight chain in good and Θ solvents. They also utilized changes in global conformation to explain these differences.

Correlation Function Shape. In all the experiments that we have performed on polyisoprene in dilute solution, the shape of the correlation function, as indicated by the ratio of τ_2/τ_1, has been essentially constant. This is true independent of the temperature, solvent power, viscosity, or solvent identity. In Table II, a collection of the corre-

Table II
Correlation Function Shapes

	τ_2/τ_1				
	2-pentanone	toluene	hexane	cyclohexane	chlorobenzene
PIP-10	3.6 ± 0.7	3.8 ± 1.1	3.6 ± 0.5	3.6 ± 0.5	
PIP-10[a]	4.3 ± 0.8	4.4 ± 1.4			
PIP-100	4.3 ± 0.9				4.6 ± 0.5
PIP-300	4.4 ± 1.0	4.6 ± 1.3			

[a] $\tau_{2,corr}/\tau_1$.

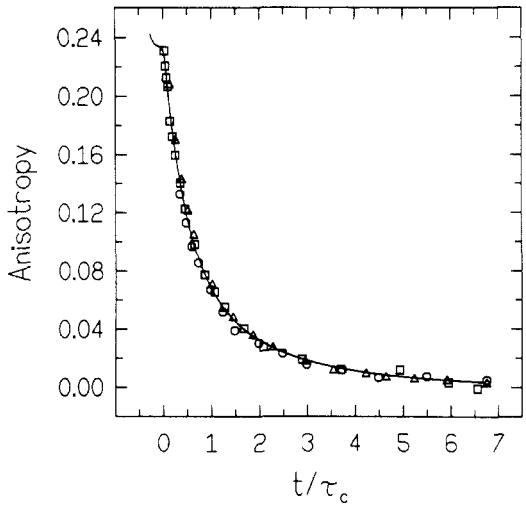

Figure 7. Constant shape of the correlation function illustrated by three time-dependent anisotropy decays for anthracene-labeled polyisoprene PIP-10 in dilute solutions of three different solvents. The anisotropy data for PIP-10 in 2-pentanone at 55 °C (○), cyclohexane at 22 °C (△), and toluene at −22 °C (□) are plotted with the time scaled by their respective correlation times: 270, 770, and 1290 ps. The smooth curve is the best fit of the Hall–Helfand correlation function to the toluene data.

lation function shapes for various molecular weight samples in different solvents is presented. To illustrate the constant shape of the correlation function visually, anisotropy data from the PIP-10 sample in three different solvents and at three different temperatures are shown in Figure 7. The time axis for each anisotropy curve has been scaled according to the fitted correlation time of the decays. As can be seen from this figure, the correlation function shapes are essentially identical. These data cover a range of temperatures from −22 to 55 °C, a range of viscosities from 0.3 to 1.1 cP, a range of correlation times from 270 to 1300 ps, and a variety of solvent types: aliphatic, aromatic, and a ketone.

Hall and Helfand derived their model for the correlation function by considering two fundamental types of conformational transitions: correlated and uncorrelated transitions.[17] The fact that the ratio of the time constants representing these processes is a constant suggests that the fundamental mechanism of local segmental dynamics in polyisoprene is the same under all conditions investigated. This observation is important for two reasons. First, it indicates that strong, specific chemical interactions are probably not dominating the dynamics of polyisoprene for the solvents we have studied. Second, it indicates that theoretical approaches which ignore the details of polymer–solvent interactions may be able to quantitatively reproduce experimental results. One such approach, Brownian dynamics computer simulations,[28] is being pursued in our laboratory on the polyisoprene system.

It should be noted that our observation that the correlation function shape is independent of solvent and viscosity in the dilute solution regime is at variance with recent work by Sasaki et al.[13] These authors utilized time-resolved fluorescence anisotropy measurements to examine the dynamics of anthracene-labeled poly(methyl methacrylate). The cause of this discrepancy is not clear at this point. These authors covered a wider range of viscosities in their study than in our work and also utilized a somewhat different form of the correlation function with a floating base line. In future work, we will explore more viscous solvents with the polyisoprene system.

Summary

The greatest strength of time-resolved optical spectroscopy as a tool for the investigation of local segmental dynamics in polymer systems is that the time dependence of the orientation autocorrelation function of a backbone bond can be directly measured. Because of this, we have been able to show directly in these experiments that the character of the motions we are measuring is not changing as the solvent, molecular weight, and temperature are varied. This allows an unambiguous comparison of the local segmental dynamics under these various conditions. Solvent quality affects local dynamics through the global chain configuration which influences the average environment of chain segments. The dependence of the local dynamics on molecular weight in good solvents and a Θ solvent supports this explanation. The excluded volume effects which tend to increase the rate of local dynamics by making the local environment of the chain segments less congested also minimize any molecular weight dependence in the observed dynamics. In contrast, the absence of strong excluded volume effects near the Θ point leads to a molecular weight dependence.

Our results are consistent with the explanation that the solvent viscosity and the solvent thermodynamic quality are sufficient to determine the local segmental dynamics of the polymer in a given solvent. We believe that by measuring both the temperature and molecular weight dependence of the local dynamics in various solvents we have provided a reasonable preliminary test of this hypothesis for the polyisoprene system. Future studies will examine this system over a wider range of viscosities and utilize additional solvents in the vicinity of the Θ temperature. Caution should be exercised in generalizing our results to other polymer systems. It might be expected that specific chemical interactions would play a greater role in more polar systems.

Acknowledgment. This research was supported by Johnson Wax and the National Science Foundation (Grant DMR-8513271). Fellowship support from Johnson Wax (P.D.H.) and Engelhard Corporation (D.A.W.) is gratefully acknowledged. We thank H. Tomonaga and N. Ota at the Toyohashi University of Technology for their help in the preparation and characterization of the labeled polymers.

Registry No. PIP, 9003-31-0.

References and Notes

(1) For example: Hedvig, P. *Dielectric Spectroscopy of Polymers*; Hilger: Bristol, 1977. Adachi, K.; Kotaka, T. *Macromolecules* **1984**, *17*, 120.

(2) For example: (a) Heatley, F. *Progress in NMR Spectroscopy* Pergamon: London, 1979; Vol. 13, p 47. Connolly, J. J.; Gordon, E.; Jones, A. A. *Macromolecules* **1984**, *17*, 722.
(3) For example: Patterson, G. D.; Stevens, J. R.; Alms, G. R.; Lindsey, C. P. *Macromolecules* **1979**, *12*, 661. Fytas, G.; Ngai, K. L. *Macromolecules* **1988**, *21*, 804.
(4) Bullock, A. T.; Cameron, G. G.; Smith, P. M. *J. Chem. Soc., Faraday Trans. 2* **1974**, *70*, 1202.
(5) Hyde, P. D.; Waldow, D. A.; Ediger, M. D.; Kitano, T.; Ito, K. *Macromolecules* **1986**, *19*, 2533.
(6) Waldow, D. A.; Hyde, P. D.; Ediger, M. D.; Kitano, T.; Ito, K. *Photophysics of Polymers*; ACS Symposium Series 358; American Chemical Society: Washington, DC, 1987; p 68.
(7) Viovy, J. L.; Monnerie, L.; Brochon, J. C. *Macromolecules* **1983**, *16*, 1845.
(8) Viovy, J. L.; Monnerie, L. *Polymer* **1986**, *27*, 181.
(9) Valeur, B.; Kasparyan, N.; Monnerie, L. *26th Int. Symp. Macromol. Mainz* **1979**, *2*, 989.
(10) Ricka, J.; Amlser, K.; Binkert, Th. *Biopolymers* **1983**, *22*, 1301.
(11) Phillips, D. *Polymer Photophysics: Luminescence, Energy Migration, and Molecular Motion in Synthetic Polymers*; Chapman and Hall: London, 1985.
(12) Sasaki, T.; Yamamoto, M.; Nishijima, Y. *Makromol. Chem. Rapid Commun.* **1986**, *7*, 345.
(13) Sasaki, T.; Yamamoto, M.; Nishijima, Y. *Macromolecules* **1988**, *21*, 610.
(14) Kivelson, D. In *Rotational Dynamics of Small and Macromolecules*; Dorfmuller, Th., Pecora, R., Eds.; Springer-Verlag: Berlin, 1987; p 1.
(15) *International Critical Tables*; McGraw-Hill: New York, 1930; Vol. 7, p 211.
(16) (a) Wagner, H. L.; Flory, P. J. *J. Chem. Phys.* **1952**, *74*, 195. (b) Poddubnyi, I. Ya., Ehrenburg, E. G. *J. Polym. Sci.* **1962**, *57*, 545. (c) Hadjichristidis, N.; Roovers, J. E. L. *J. Polym. Sci.* **1974**, *12*, 2521.
(17) Hall, C. K.; Helfand, E. *J. Chem. Phys.* **1982**, *77*, 3275.
(18) Kubo, R.; Toda, M.; Hashitsume, H. *Statistical Physics II: Nonequilibrium statistical Mechanics*; Springer-Verlag: Berlin, 1985; p 42.
(19) *Polymer Handbook*, 2nd ed.; Brandrup, J., Immergut, E. H., Eds.; Wiley: New York, 1975.
(20) Bauer, D. R.; Brauman, J. I.; Pecora, R. *Macromolecules* **1975**, *8*, 443.
(21) (a) Riseman, J.; Kirkwood, J. G. *J. Chem. Phys.* **1949**, *17*, 442. (b) Zimm, B. H. *J. Chem. Phys.* **1956**, *24*, 269. (c) Isihara, A. *J. Chem. Phys.* **1967**, *47*, 3821.
(22) Flory, P. J. *Statistical Mechanics of Chain Molecules*; Wiley Interscience: New York, 1969; p 52.
(23) Waldow, D. A.; Johnson, B. S.; Babiarz, C. L.; Ediger, M. D.; Kitano, T.; Ito, K. *Polym. Commun.* **1988**, *29*, 296.
(24) The self-avoiding random walk utilized six possible step directions of equal probability. If any given step visited a site previously visited, the walk was thrown out and restarted. For self-avoiding walks greater than 48 segments, the enrichment method of Wall and Erpenbeck was utilized (Wall, F. T.; Erpenbeck, J. J. *J. Chem. Phys.* **1959**, *30*(3), 634).
(25) For a general discussion of the use of random walk models for good and Θ solvent conditions, see: de Gennes, P.-G. *Scaling Concepts in Polymer Physics*; Cornell University Press: Ithaca, NY, 1979; p 29.
(26) Schaefer, D. W.; Han, C. C. *Dynamic Light Scattering*; Pecora, R., Ed.; Plenum: New York, 1985; p 181.
(27) Heatley, F.; Begum, G. *Polymer* **1976**, *17*, 399.
(28) Weber, T. A.; Helfand, E. *J. Phys. Chem.* **1983**, *87*, 2881.

Dynamics of Gel Electrophoresis

Edward O. Shaffer II and Monica Olvera de la Cruz*

Department of Materials Science and Engineering, Northwestern University, Evanston, Illinois 60208. *Received May 19, 1988; Revised Manuscript Received August 18, 1988*

ABSTRACT: An off-lattice computer simulation based on the Langevin equation of motion is used to study gel electrophoresis. The simulated chain dynamics are dramatically different from the dynamics predicted by tube-reptation theories. The mobility of different length chains is traced, showing the loss of length dependence as the field is increased. The dynamics of the chain in the field-independent mobility regime are illustrated.

Introduction

Gel electrophoresis has great importance in modern molecular biology as a method for separating proteins and nucleic acids, in particular DNA. In its simplest form, the technique consists of applying a constant electric field to a gel that contains the molecules of interest. In the limit of small electric fields, the mobility of linear polymer chains is inversely dependent on length. After a period of time, the chains of different sizes separate physically in the gel. Unfortunately, for higher electric fields, the inverse length dependence of the mobility is strongly reduced. This loss of length-dependent mobility occurs at smaller fields for larger chains. Consequently, the technique is unable to separate very long chains.[1] In an effort to optimize the separation process, more sophisticated approaches have been developed.[2,3] Despite the importance of gel electrophoresis, the dynamics of this process are still not fully understood. Experimental developments have relied solely on empirical observations.

In order to understand the dynamics of gel electrophoresis and why the mobility loses its inverse length dependence, we have developed an off-lattice computer program of the process. The results of the simulation illustrate a diffusional process not explained by the existing tube-reptation theories of gel electrophoresis.[4,5]

de Gennes[6a] introduced the reptation model to explain the dynamics of long linear chains in a gel with no applied forces. The diffusion of an ideal chain of N units of length b is restricted by the gel. The reptation model accounts for this restriction by confining the polymer to diffuse along the random path of a tube. The tube's diameter is the average distance between network junction points, a. For distances less than the tube diameter, a, the polymer moves freely. For larger distances, the chain is constrained to diffuse along the tube path. The tube consists of N' segments of length a where $N' = Nb^2/a^2$. The contour length of the tube, L, is given by

$$L = N'a \tag{1}$$

In tube-reptation theories, for diffusion larger than the tube diameter, all the lateral motion perpendicular to the tube is explicitly ignored. Only the end tube segments are free to move. As a result, the path of the chain is determined by the end tube segments.

Current gel electrophoretic theories are based on the tube-reptation concept constraining the chain to move

0024-9297/89/2222-1351$01.50/0